Proceedings of the Research Institute of Atmospherics,
Nagoya University, vol. 37 (1990) –Research Report–

A Digital Processing for Analogue Geomagnetic Records

K. Kurahashi, K. Ohta, T. Watanabe, T. Ogino
A. Iwata, N. Nishitani, T. Takayanagi, and K. Yumoto
The Research Institute of Atmospherics, Nagoya University
Toyokawa, Aichi 442, Japan

T. Saito
Onagawa Magnetic Observatory & Geophysical Institute
Tohoku University, Sendai 980, Japan

Abstract

A data base system is developed for utilizing long term, analogue data stored for many years in the light of modern analysis. As an example, analogue magnetic records of an induction magnetometer at Onagawa Magnetic Observatory are digitized and processed. Frequency-time spectrograms are derived by Fourier transformation of the digitized data, and, $\Sigma Kc3$ and $\Sigma Ki2$ indices, that show average pulsation activities in the Pc3 and Pi2 frequency ranges, are calculated. These indices are compared with magnetic field variations measured by GOES–5 synchronous satellite and the solar wind velocity observed by IMP–8 satellite. These comparisons are useful for general view of the solar wind-magnetospheric interaction.

1. Introduction

A certain phenomenon observed in space environment normally involves various effects from numerous physical processes occurring around the observation point. It is thus useful to compare an observation with other related quantities and to find out

essential relationships among them to make a better comprehension of the relevant processes.

It is evident that the machine readable data base is an essential requirement for the comparison. Especially, the construction of digital data base from analogue data obtained for many years is extremely useful in studying long term variations in any fields. We are now assembling a new system for data managements including an analogue-digital conversion, frequency-time spectrograms and real-time two dimensional data processing. A step of the system assembling, as well as the initial result, is described in this paper.

2. Data sets

As an example, the material used here is an induction magnetogram recorded on an FM magnetic tape. The records were obtained for a period of twenty years at the Onagawa Magnetic Observatory (ONW), Tohoku University (magnetic latitude $\Phi = 28.3°$, magnetic longitude $\Lambda = 206.8°$, $L \simeq UT + 9.0$ hr; see Saito, 1976) using a 2m core-type induction magnetometer. Four tracks of the tape were allocated as, #1 for dZ/dt, #2 for dH/dt, #3 for dD/dt and #4 for time marks. Two kind time marks were given on the track #4. One was for each one minute, and the other was for each 10 minutes. The recording speed was 0.003 ips. This slow speed recording enabled the system to cover two weeks with one roll of magnetic tape.

In addition to the induction magnetograms from ONW station, we use here magnetic field data obtained by GOES–5 synchronous satellite, and solar wind velocity measured by IMP–8, for studying the relationships.

3. Analog-Digital Conversion

The original FM data of the induction magnetogram at ONW are first reproduced by an FM reproducer. The reproducing speed is 3 ips: this is one thousand times of the original recording speed. This is extremely useful for the fast analysis. Reproduced data are led to an Analogue-Digital Converter, which consists of a Minicomputer (MS 120), and then digitized at a sampling rate of 1 KHz. This corresponds to the sampling rate of 1 Hz in the original time base. The converted digital data are then stored on the other magnetic tape for further analysis.

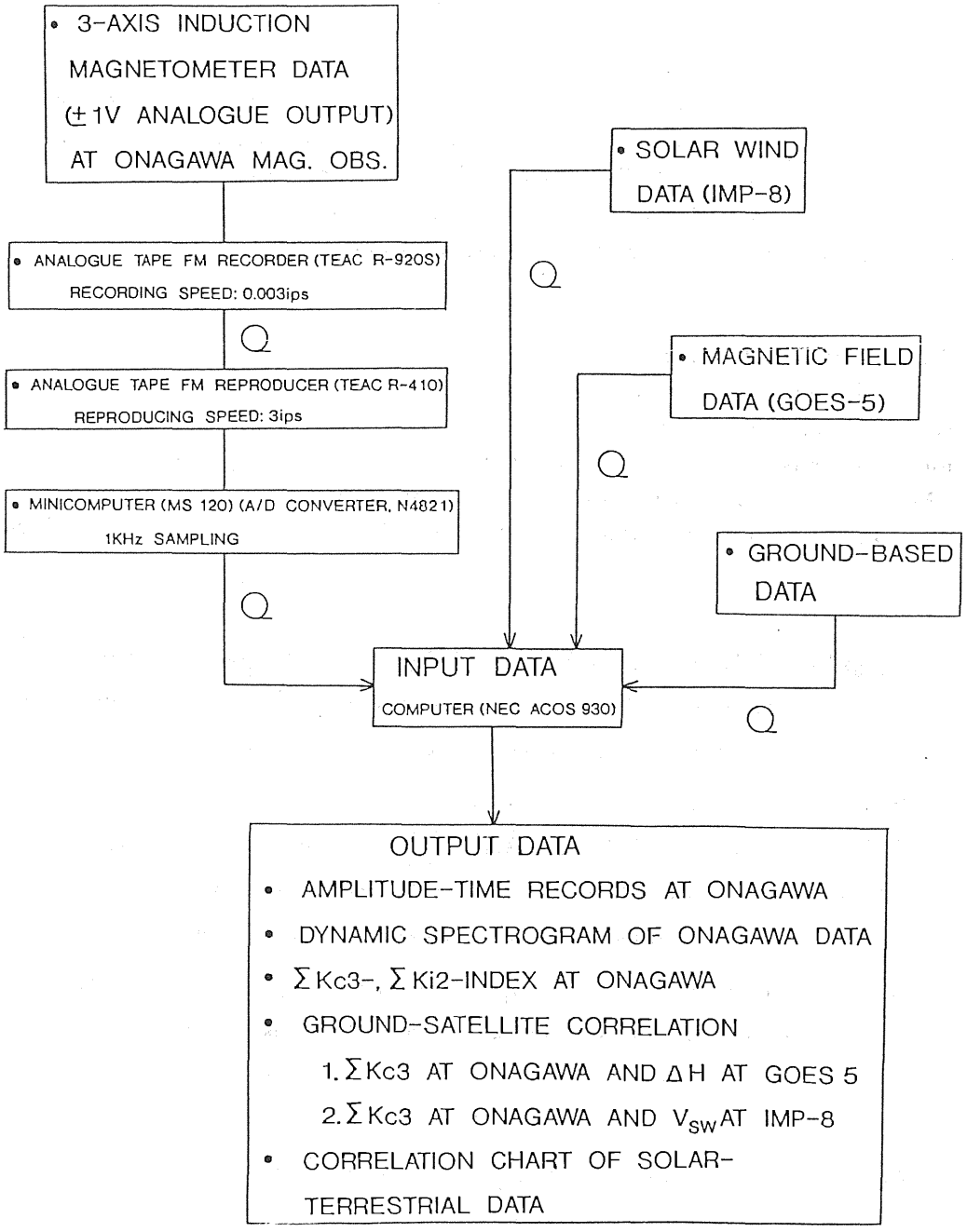

Fig. 1. Flow chart of data processing. The digitized geomagnetic data and the referential data from satellites are collected to the central part, indicated by INPUT DATA., and by the comparison and reduction of these data, the items of OUTPUT DATA are obtained.

4. Data Processing

A flow chart of the data processing is shown in Figure 1. The central part, indicated by INPUT DATA, shows the inflow of the converted digital data and the referential data from satellites. After elimination of noise and correction of time, these data are converted to the OUTPUT DATA items on the chart. Details of each procedure are mentioned in the following subsections.

4.1 Reductions of Amplitude-Time Records.

The converted digital data mentioned in the previous section have the following two problems: (1) shifts of time records, and (2) contamination due to noise. The former is caused by the difference in clock of the recording system and that of the FM reproducer. The latter comes from the original records.

Figure 2 shows an example of amplitude-time display of magnetic field changes

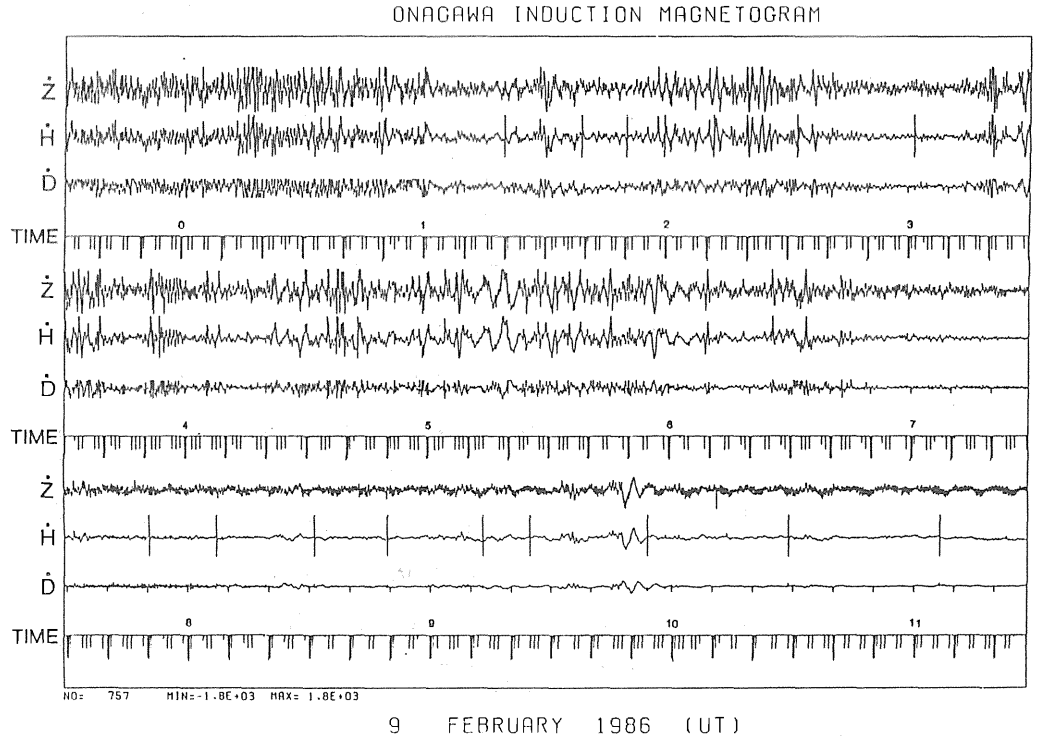

Fig. 2. An example of converted digital data: amplitude-time record during the morning period on February 9, 1986. The numbers denoted on the time record indicate hours. Accompanying spike-like noise, especially 7–12 hours in the H component, and shifts of time mark.

and time marks, reproduced from the digitized data, during the morning period on February 9, 1986. The numbers denoted on the time record indicate hours. The thick vertical lines below are 10-minutes time marks. The 10-minutes time marks consist of 300 Hz sinusoidal waves recorded for 40 second each 10 minutes. Between them we see spike-like 1-minute time marks, but some are missing. This is because the duration of the 1-minute time mark is less than 1 second, and therefore, 1 second sampling could miss the time signal when the phase of the sampling deviates from the record.

Since the beginning of the 10-minute time marks are determined within 1 second accuracy, we conventionally assume that the first sampling time of each 10-minutes time mark is accurate. Then, we can determine the "accurate" time of each sampling in reference of each 10-minutes timing. The procedure to do so is as in the following. The sampling number should be 600 for each 10-minutes time mark if the timing system of both recording and the reproducing system is identical, but actually this is not the case. Therefore we count the sampling number between successive 10-minutes time marks. Then each sample is labeled with a time which is adjusted with 600/(sample number).

In the next step, we eliminate the artificial noise in the records. Some of the spike-like noise in the channel 3 for the geomagnetic component $\dot{H}(= dH/dt)$ are from

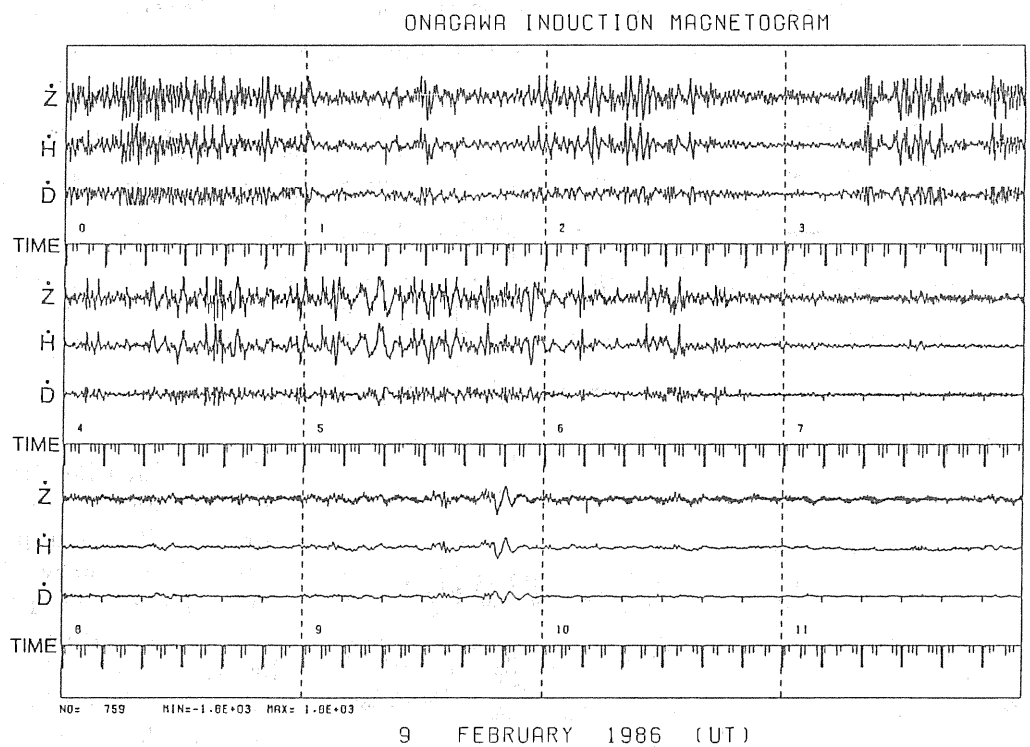

Fig. 3. The reduced form of Fig. 2. The noise is eliminated and the shifts of time mark are corrected.

the original analogue record. Since the noise shows a very sharp increase and decrease in the signal level, it is possible to eliminate the noise through the following procedure. First, we arbitrarily set the amount of $\Delta An/\Delta T$, which denotes the increment of amplitude versus time. The time variations faster than the preset amount are eliminated, then the gaps are filled by interpolated values by using the levels immediately before and after the eliminated data point. An optimum value for $\Delta An/\Delta T$ is determined in the "trial and error" manner, in order to avoid an elimination of rapidly varying signals during a strong magnetic storm. The reduced data are shown in Figure 3. The noise of $\dot{D}(= dD/dt)$ component synchronizing with the time marks cannot be perfectly eliminated. To attain a sufficient reduction of this noise we must set $\Delta An/\Delta T$ to a lower level value. However, this may lead to the removal of small amplitude signals. This point will be improved in a near future. As seen later, the production on the $\Sigma Kc3$ and $\Sigma Ki2$ indices are based upon the $\dot{H}$ component data in which the noise are well eliminated. All the reduced data are stored on magnetic tape.

4.2 Identification of Geomagnetic Events

The results above are first used to make up identification of a geomagnetic events. The arrows shown in Figure 4 express the onset of characteristic events of Pi 2 and Si+, whose onset time are given in the upper right column. The depiction

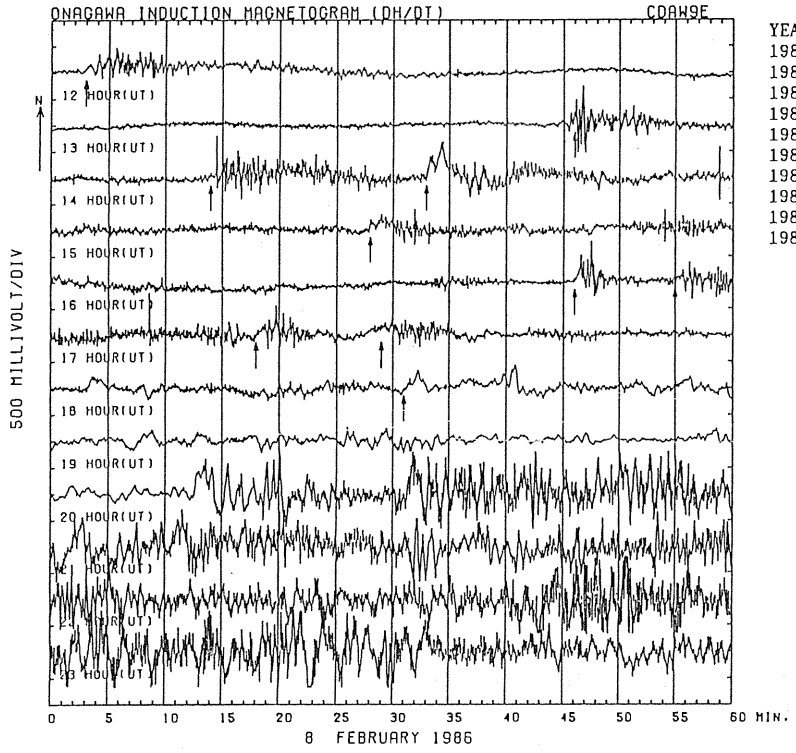

YEAR	MONTH	DAY	HOUR	MINUTE	EVENT
1986	2	8	12	3	PI2
1986	2	8	13	46	PI2
1986	2	8	14	14	PI2
1986	2	8	14	33	SI+
1986	2	8	15	28	PI2
1986	2	8	16	46	PI2
1986	2	8	16	55	PI2
1986	2	8	17	18	PI2
1986	2	8	17	29	PI2
1986	2	8	18	31	SI+

Fig. 4. Identification of geomagnetic events for the afternoon period of February 8, 1986. The onsets of Pi 2 and Si+ are shown by the arrow signs. Time records are indicated in the margin.

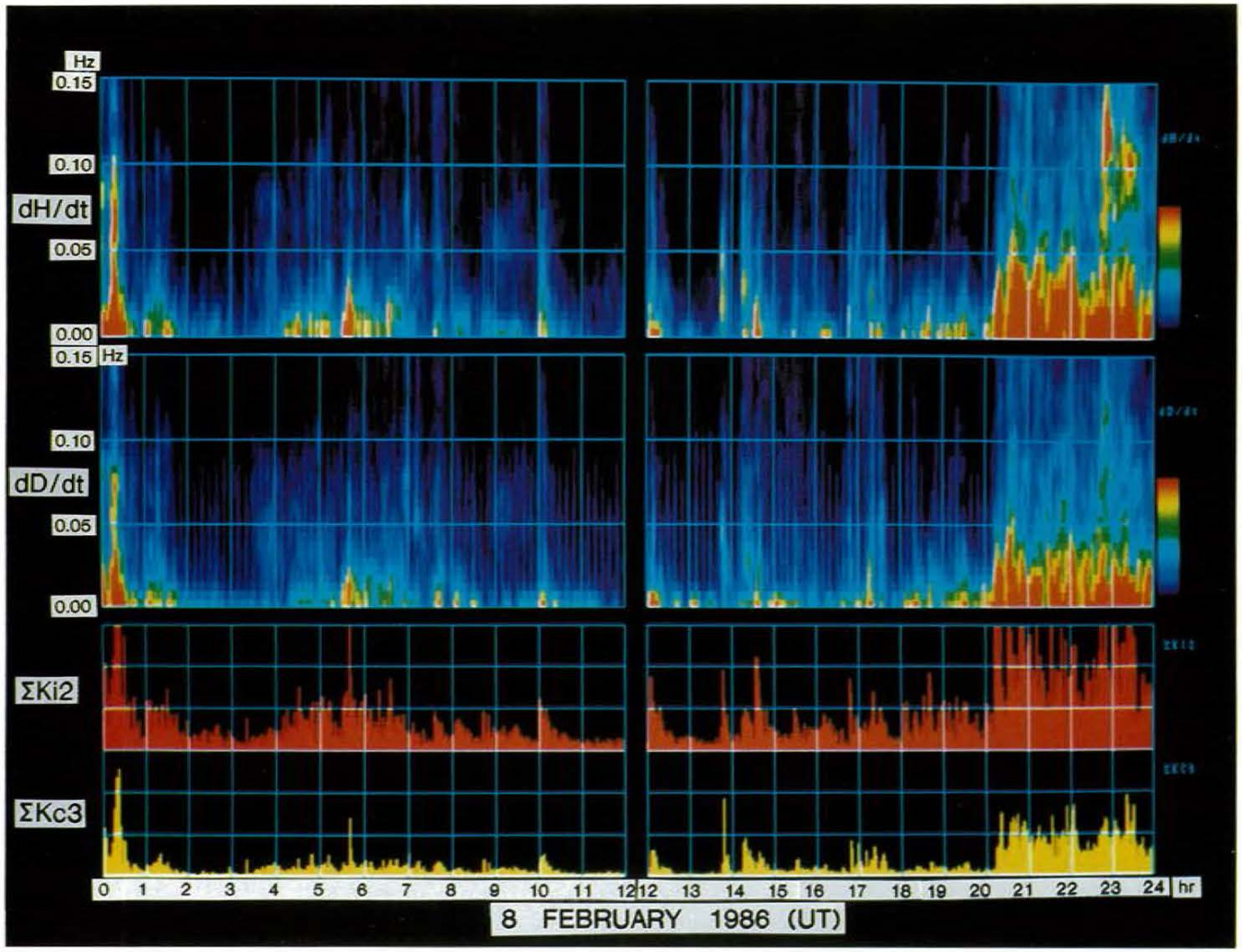

Fig. 5. Frequency-time spectrograms of the geomagnetic pulsations and the $\Sigma Kc3$, $\Sigma Ki2$ index (for 8 February 1986). These indices are defined as the average wave intensity of Pc 3 and Pi 2 frequency ranges, respectively, and derived from dH/dt component of the frequency-time spectrograms. The wave intensity is illustrated by the color code from red (the strongest intensity) to blue (the weakest intensity), as shown in right hand of figures.

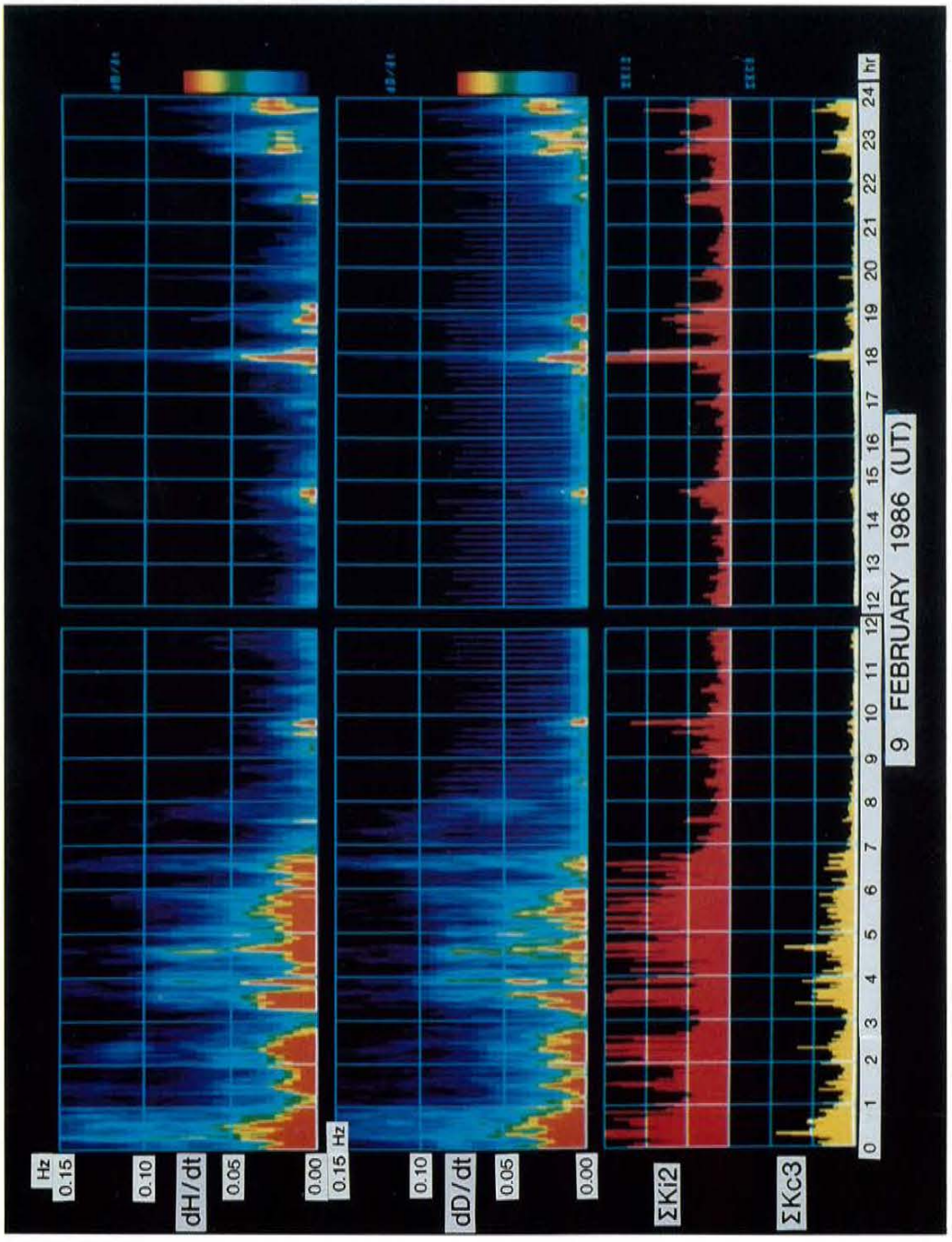

Fig. 6. Same as Fig. 5 (for 9 February 1986).

of Pi 2, Si+ and the other event are given in the literature, for example, Saito, 1969; Araki, 1977; and Nishida, 1978. The time-amplitude records are $\dot{H}$ component during the afternoon period of February 8, 1986, when a large geomagnetic storm occurred. The sudden commencement time is at 20 h 13 m UT. The display is available for any 12 hours intervals selecting time intervals for the convenience of "event" display.

4.3 Frequency-Time Spectrograms of Geomagnetic Pulsations and $\Sigma Kc3$-, $\Sigma Ki2$ -indices.

The amplitude-time records are Fourier transformed and represented by frequency-time spectrograms. The color display of dH/dt and dD/dt in Figures 5 and 6 shows the frequency-time spectrograms for 0–24 hours of 8 and 9 February 1986, respectively. In these figures, the frequency range of full scale with 0–0.15 Hz covers the Pc 3 (0.02–0.10 Hz, 10–50 sec.) and the Pi 2 (0.0067–0.025 Hz, 40–150 sec.) ranges of geomagnetic pulsations. The wave intensity is illustrated by means of the color code from red (the strongest intensity) to blue (the weakest intensity), as shown in right hand of the figures. Subsequently, the averaged wave intensity in Pc 3 and Pi 2 ranges, which we define as the $\Sigma Kc3$ and $\Sigma Ki2$ indices, respectively, have been obtained by summing up the intensity of frequency-time spectrograms within each frequency range. The time resolution in Figures 5 and 6 is one minute and forty seconds.

4.4 Comparison with Magnetic Field Variations at the GOES-5 Satellite.

In order to demonstrate the usefulness of $\Sigma Kc3$ and $\Sigma Ki2$ indices, we compare these indices with GOES-5 satellite data (L = 6.6, $\lambda = 74°$W, MLT$\simeq$ UT+19.0 hr). Simultaneous magnetic field variations at GOES-5 on February 8, 1986 are shown in Figure 7 along with the frequency-time spectrograms and pulsation indices. H(NT),V(NT) and D(NT) are parallel to dipole, radially outward and azimuthal components measured in nano-tesla units, respectively. The satellite sometimes entered the magnetosheath on February 8, 1986, exhibited in the H component records with the shaded area. It is found that the satellite repeatedly went "in and out" of the magnetosheath after the storm sudden commencement according to the rapid change of the solar wind dynamic pressure. Details on these physics and correlation with the $\Sigma Kc3$ and/or $\Sigma Ki2$ indices are in the investigation.

4.5 Correlation between $\Sigma Kc3$ Index and Solar Wind Velocity at IMP-8 Satellite.

Many authors have studied the generation and propagation mechanisms of Pc 3 hydromagnetic waves (see review by Odera, 1986; Yumoto, 1986). It is generally believed that Pc 3 waves are "exogenic" pulsations which are continuously V_{SW}

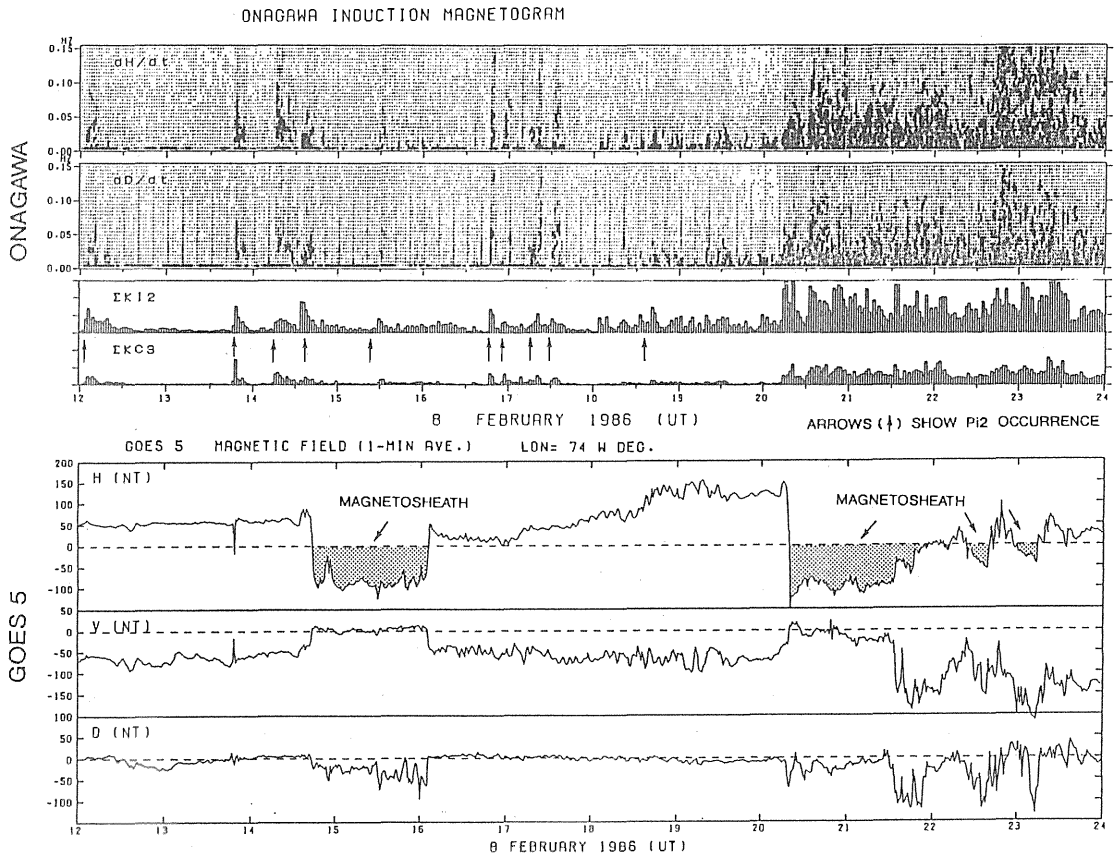

Fig. 7. Comparison between the magnetic activity at Onagawa and the magnetic field variations at GOES–5. Geosynchronous orbital satellite GOES–5 often entered the magnetosheath (illustrated by shaded area for H component) and repeatedly went "in and out" at storm time on the afternoon of February 8, 1986.

driven in the regions near the bow shock by the interaction between the solar wind and the magnetosphere, and that these waves penetrate into the magnetosphere through some mechanisms. However, it has not yet been well understood how these can be transmitted into the low-latitude ionosphere. Pc 3 pulsations observed on the ground are controlled by the solar wind parameters and the magnitude of the interplanetary magnetic field (see for example, Wolfe, 1980; Russell and Hoppe, 1981; Yumoto *et al.*, 1984). A good correlation between the Pc 3 pulsations and the solar wind velocity was demonstrated by several authors (Wolfe, 1980; Odera, 1986). Investigations of the correlation between the $\Sigma Kc3$ index and the solar wind parameters using a large amount of data will give much information on long-term dependences on the solar wind and the interplanetary magnetic field.

As a preliminary study, we examine relations between the solar wind velocity (hereafter denoted V_{SW}) and $\Sigma Kc3$ index. The V_{SW} was obtained from the IMP–8 satellite. Typical examples of the results are illustrated for two specific intervals in

Figures 8 and 9, respectively. The former is for February 1986, when the storm was observed; the latter is for May 1986, when a weak geomagnetic activity was obtained. It is believed in general that Pc3 pulsations arise in the daytime, and thus we used the pulsation data obtained in the local time (LT) interval from 5:00 to 16:00 at ONW, which is 20–07 in UT. Since Vsw from IMP–8 is one-hour averaged data, $\Sigma Kc3$ in Figures 5 and 6 are also integrated and averaged for one hour. As the IMP–8 had a perigee of 23.1Re and apogee of 46.3 Re, where Re is the earth's radius, the propagation time of Pc 3 waves from the position of IMP–8 to ONW with near the Alfvén velocity ought to attain from five to twenty minutes. As the statistics in February and May 1986 appear to be insufficient, we don't draw a regression line. However, a general tendency, *i.e.*, " $\Sigma Kc3$ increases with V_{SW}" is evident. The larger amount of data will give a clearer picture of the relationships. The comparisons of these data, measured in the interplanetary space and on the ground (ONW) will give some clues to the transport process of the solar wind HM energy into the magnetosphere.

5 Summary and Conclusions.

One of our main intention is to utilize large amount of analogue data obtained in the past in the light of a new physical idea. Data processing of the geomagnetic records here is an example. The original analogue data, from the Onagawa Magnetic Observatory, Tohoku University, have been digitized with high-time resolution for computer analysis. A program for removing the noise and adjusting the time shifts has been developed by examining the specific characteristics of noise and time record. This program can be applied for similar analogue-digital conversion. The amplitude-time records are transformed to the frequency-time spectrograms, and thereby we calculate the $\Sigma Kc3$ and $\Sigma Ki2$ indices which express the averaged value of the wave intensity in the Pc 3 and Pi 2 frequency ranges. These indices are useful for research on the energy transfer process from the solar wind into the magnetosphere, as well as monitoring the interplanetary and magnetospheric disturbances.

A comparison between $\Sigma Kc3$ index at ONW and magnetic variations at GOES–5 satellite was attempted. We suppose that such examination is useful for the study on the solar wind-magnetosphere interaction. The relation of $\Sigma Kc3$ with the solar wind velocity at IMP–8 satellite was also obtained. It was confirmed that the $\Sigma Kc3$ index has a tendency to increase with the solar wind velocity. Further statistical analysis of larger amount of data will be efficient to establish the relationship. Although $\Sigma Ki2$ index was not investigated in this paper, it will be useful for study on the magnetospheric substorm, because Pi 2 pulsations are a transient hydromagnetic signal associated with the substorm expansion and/or intensification.

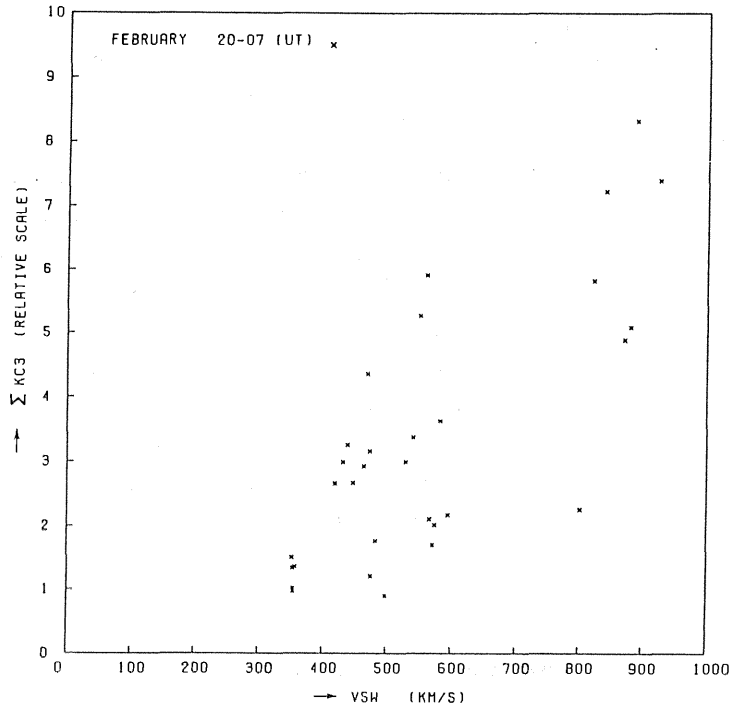

Fig. 8. Correlation between the $\Sigma Kc3$ index and the solar wind velocity at IMP–8. Correlation values are plotted for all data observed in the daytime during February 1986. 20–07(UT) noted in the upper part correspond to 5–16(LT) at Onagawa.

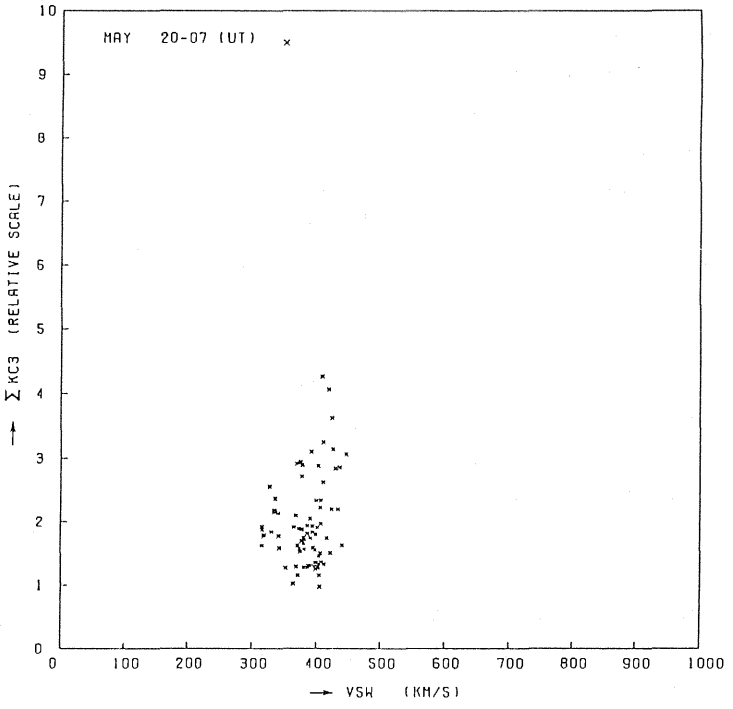

Fig. 9. Same as Fig. 8 (for May 1986).

Acknowledgements

The authors wish to thank Prof. T. Oguti, Director of The Research Institute of Atmospherics, Nagoya University, for his encouragement and interest in this work.

References

Araki, T., Global structure of geomagnetic sudden commencements, *Planet. Space Scie.*, ***25***, 373, 1977.

Nishida, A., Geomagnetic Diagnosis of the Magnetosphere, *Springer-Verlag*, 1978.

Odera, T. J., Solar wind controlled pulsations: a review, *Rev. Geophys.*, ***24***, 55, 1986.

Russell, C. T., and M. M. Hoppe, The dependence of upstream wave periods on the interplanetary magnetic field strength, *Geophys. Res. Lett.*, ***8***, 615, 1981.

Saito, T., Geomagnetic pulsations, *Space Scie. Rev.*, ***10***, 319, 1969.

Saito, T., The Hissa (High-Speed Spectrum Analysis) method to analyze various time-varying phenomena in space physics, *Rept. Ionos. Space Res., Jap.*, ***30***, 69, 1976.

Wolfe, A., Dependence of mid-latitude hydromagnetic energy spectra on solar wind speed and interplanetary magnetic field direction, *J. Geophys. Res.*, ***85***, 5977, 1980.

Yumoto, K., T. Saito, B. T. Tsurutani, E. J. Smith, and S.-I. Akasofu, Relationship between the IMF magnitude and Pc3 magnetic pulsations in the magnetosphere. *J. Geophys. Res.*, ***89***, 9731, 1984.

Yumoto, K., Generation and propagation mechanisms of low-latitude magnetic pulsations – a review, *J. Geophys.*, ***60***, 79, 1986.